Monitoring the reaction of carbachol with acetylcholinesterase by thioflavin T fluorescence and acetylthiocholine hydrolysis

Terrone L. Rosenberry, **Leilani K. Sonoda**, **Sarah E. Dekat**, **Bernadette Cusack**, and **Joseph L. Johnson**

Mayo Clinic College of Medicine, Departments of Neuroscience and Pharmacology, Jacksonville, Florida, 32224

Abstract

Acetylcholinesterase (AChE) contains a narrow and deep active site gorge with two sites of ligand binding, an acylation site (or A-site) at the base of the gorge and a peripheral site (or P-site) near the gorge entrance. The P-site contributes to catalytic efficiency by transiently binding substrates on their way to the acylation site, where a short-lived acyl enzyme intermediate is produced. Carbamates are very poor substrates that, like other AChE substrates, form an initial enzyme-substrate complex and proceed to an acylated enzyme intermediate which is then hydrolyzed. However, the hydrolysis of the carbamoylated enzyme is slow enough to resolve the acylation and deacylation steps on the catalytic pathway. Here we show that the reaction of carbachol (carbamoylcholine) with AChE can be monitored both with acetylthiocholine as a reporter substrate and with thioflavin T as a fluorescent reporter group. The fluorescence of thioflavin T is strongly enhanced when it binds to the P-site of AChE, and this fluorescence is partially quenched when a second ligand binds to the A-site to form a ternary complex. These fluorescence changes allow not only the monitoring of the course of the carbamoylation reaction but also the determination of carbachol affinities for the A- and P-sites.

Keywords

Acetylcholinesterase; thioflavin T; carbamoylation; peripheral site; enzyme mechanism

INTRODUCTION

Acetylcholinesterase (AChE)[1] hydrolyzes the neurotransmitter acetylcholine at one of the highest known enzymatic rates (1). Partial inhibition of AChE activity in the brain, obtained with a number of inhibitors including carbamoyl esters, has been shown to have therapeutic benefits. AChE inhibitors that penetrate the blood-brain barrier elevate the levels of endogenous acetylcholine and are useful in the symptomatic treatment of Alzheimer's disease (2). However, complete inactivation of AChE, which can occur with organophosphate chemical warfare agents (3), leads to toxic accumulation of acetylcholine and failure of

Corresponding author: Terrone L. Rosenberry, Ph.D, Mayo Clinic, 4500 San Pablo Road, Jacksonville, FL 32224, e-mail: rosenberry@mayo.edu, FAX: (904) 953-7370, Phone: (904) 953-7375.

[1]Abbreviations: AChE, acetylcholinesterase; ATMA, 3-(acetamido)-*N,N,N*-trimethylanilinium; DTNB, 5,5'-dithiobis-(2-nitrobenzoic acid); TMTFA, *m*-(*N,N,N*-trimethylammonio) trifluoroacetophenone.

cholinergic synaptic transmission, with consequent deterioration of neuromuscular junctions, flaccid muscle paralysis, and seizures in the central nervous system.

An essential feature of AChE activity at many synapses is the ability to hydrolyze acetylcholine within a millisecond of its release (4). Insights into this high catalytic efficiency were obtained from ligand binding studies (5–7) and X-ray crystallography (8), which revealed a narrow active site gorge some 20 Å deep with two separate ligand binding sites. At the base of the gorge is the acylation or A-site where residue W86 [2] binds the trimethylammonium group of acetylcholine and H447, E334, and S203 participate in a triad that catalyzes the transient acylation and deacylation of S203 during each substrate turnover. The peripheral or P-site, spanned by residues W286 near the mouth of the gorge and D74 near a constriction at the boundary between the P-site and the A-site, specifically binds certain ligands like the neurotoxin fasciculin (9,10)] and the fluorescent probes propidium (6) and thioflavin T (7).

Detailed information about the AChE catalytic mechanism can be obtained by characterizing intermediates formed on the catalytic pathway. A class of AChE inhibitors comprised of carbamoyl esters (here referred to as carbamates) is particularly useful in this regard. Carbamates are actually very poor substrates for AChE. Like other AChE substrates, they form an initial enzyme-substrate complex ES and proceed to an acylated enzyme intermediate which is then hydrolyzed. However, unlike carboxylic acid ester substrates, the hydrolysis of the carbamoylated enzyme is slow enough to resolve the acylation and deacylation steps. Despite this striking advantage offered by carbamates, few comprehensive analyses of their reactions with AChE have been undertaken. Here we report on the interaction of AChE with carbachol, a carbamate whose reaction mechanism with AChE is important because it is an isosteric analog of acetylcholine. We show that the reaction of carbachol with AChE can be monitored both with acetylthiocholine as a reporter substrate and with thioflavin T (Figure 1) as a fluorescent reporter group. The fluorescence of thioflavin T is strongly enhanced when it binds to the P-site of AChE, and this fluorescence is partially quenched when a second ligand binds to the A-site to form a ternary complex (7). In addition to monitoring the course of the carbamoylation reaction, we show that these fluorescence changes allow the determination of carbachol affinities for the A- and P-sites.

Experimental Methods

Materials

Recombinant human AChE was expressed as a secreted, disulfide-linked dimer in *Drosophila* S2 cells and purified as outlined previously (11). Thioflavin T and carbachol (carbamoylcholine chloride) were from Sigma. Thioflavin T was recrystallized from water, and concentrations were assigned by absorbance at 412 nm with $\varepsilon_{412\,nm} = 36{,}000$ M^{-1}cm^{-1}.

Steady-State Measurements of AChE-Catalyzed Acetylthiocholine Hydrolysis

Hydrolysis rates v for acetylthiocholine were measured by spectrophotometry in a coupled reaction in which thiocholine generated in the presence of DTNB was determined by formation of the thiolate dianion of DTNB at 412 nm ($\Delta\varepsilon_{412\,nm} = 14{,}150$ M^{-1}cm^{-1}) (12). Total AChE concentrations (E_{tot}) were calculated assuming 450 units/nmol (7).[3]

---

[2]Throughout this paper we number amino acid residues according to the human AChE sequence.

[3]One unit of AChE activity corresponds to 1 μmol of acetylthiocholine hydrolyzed/min under standard pH-stat assay conditions at pH 8 (7). Our conventional spectrophotometric assay at 412nm is conducted in pH 7 buffer. With wild type AChE and 0.5 mM acetylthiocholine, this assay results in 4.8 $\Delta A_{412\,nm}$/min with 1 nM AChE or about 76 % of the pH stat assay standard.

Stopped-Flow Measurements of Carbachol Reaction with AChE

Stopped-flow methods were applied to measure the approach to the carbamoylation steady state with acetylthiocholine as a chromogenic reporter substrate or thioflavin T as a fluorescent reporter ligand. Absorbance was monitored on a Varian Cary 3 Bio UV Visible spectrophotometer at 412 nm and fluorescence, on a Perkin-Elmer LS-50B luminescence spectrometer, both thermostatted at 25 °C. Fluorescence excitation was at 450 nm and emission at 490 nm, with excitation and emission slits of 10 to 20 nm. A thermostatted Hi-Tech SFA 20 stopped flow apparatus was used to rapidly mix equal volumes (300 ul) of AChE in one syringe and carbachol in the other. Measurements were recorded at fixed intervals as short as 33 msec (absorbance) or 20 msec (fluorescence). Acetylthiocholine as the reporter substrate and DTNB were added only to the carbachol syringe, but with a DTNB concentration after mixing of 10 mM to insure that its reaction with thiocholine was not rate limiting during the absorbance increase. The solution was buffered to pH 7.0 with a total of 30 mM phosphate and 70 mM Na^+ (added as Na_2PO_4 and NaOH). Thioflavin T as the reporter was added at equal concentrations to both syringes in 40 mM sodium phosphate, 0.04% Triton X-100 at pH 7.0. To maintain constant ionic strength when the range of carbachol concentrations extended to 60 mM, additional NaCl was included added so that the sum of the carbachol and NaCl concentrations was 60 mM.

A two-site model of carbamoylation of AChE in the presence of a reporter substrate

With carbamate substrates, both the formation and hydrolysis of the acylated enzyme intermediate, or carbamoyl enzyme (EC), are slow enough to allow equilibrium assumptions. A general approach is given in Scheme 1 (13,14).

In this scheme, k_{12} is the overall carbamoylation rate constant and k_{21} is the overall decarbamoylation rate constant. P and COH are the products released during the carbamoylation and decarbamoylation reactions, respectively. The terms $E{\cdot}L$ and $EC{\cdot}N$ represent all species in equilibrium with E and EC, respectively (*i.e.*, $[E]{\cdot}L + [EC]{\cdot}N = E_{tot}$, where $[E]$ and $[EC]$ are the respective concentrations of E and EC and E_{tot} is the total concentration of enzyme active sites), and L and N are sums of terms (involving rate and equilibrium constants and ligand concentrations) that depend on the details of a selected reaction scheme. The rate equation corresponding to Scheme 1 can be solved explicitly if all ligand concentrations remain essentially constant over the reaction time course (13,15), as recently described (14).

In the simplest application of Scheme 1, a fluorogenic carbamate releases a fluorescent product P and the only enzyme intermediates involve the carbamate (13,14). Alternatively, reactions of a carbamate S_1 can be measured with a chromogenic reporter substrate S_2 like acetylthiocholine that generates a hydrolysis product P_2. Scheme 1 still provides an appropriate framework for analysis, but the expressions for L and N now include enzyme species with bound S_2 as well as bound S_1. A useful solution (eq. 1) resolves k_{12} and k_{21} and here is restricted to the case when $[EC] = 0$ at time t = 0.[4]

$$[P_2] = \left(\frac{v_0}{(k_{12}+k_{21})}\right)\left[k_{21}t + \left(\frac{k_{12}}{k_{12}+k_{21}}\right)\left(1 - e^{-[(k_{12}+k_{21})t]}\right)\right] + [P_2]_{(t=0)}$$

(eq. 1)

Carbamate reactions with AChE can be analyzed according to Scheme 1 and fitted directly to eq. 1 to obtain values of the overall rate constants k_{12} and k_{21} (14). However, slightly better fits were obtained when the rate equations corresponding to Scheme 1 were solved directly by the numerical integration program SCoP (Simulation Resources, Inc., Redlands, CA; version

---

[4]Similar solutions have been derived previously: reference Rosenberry, T. L. (1969), Ph.D. Dissertation, The University of Oregon, Eugene, OR; (16,14).

3.52) that we have used previously (12,17). This program allows ligand concentrations to vary over the reaction time course, and it thereby permits analysis at low concentrations of S_2 to minimize the contributions of terms with S_2 to expressions for k_{12} and k_{21}. These expressions, which depend on derivations of L and N for a selected reaction scheme like Scheme 2 below (e.g., 14), provide much mechanistic insight but will not be considered further in this report. The SCoP program also permitted incorporation of a slower component of relatively small exponential amplitude (~ 5% of the total) that was observed in virtually all reactions regardless of the carbamate (T.L. Rosenberry, manuscript in preparation).

One model for the reaction of carbamate substrates with AChE is presented in Scheme 2 (14).

This scheme includes an initial complex with substrate bound to the P-site (ES_P, where the subscript P denotes the ligand bound to the P-site) and a subsequent complex with substrate shifted to the A-site (ES) where formation of the carbamoylated enzyme (EC) occurs. Ternary complexes in which intermediates also bind substrate at the P-site (ESS_P and ECS_P) allow the rate constants for conversion of one intermediate to the next to be altered by the relative factors a or b, respectively.

Determination of ligand affinities for the A- and P-sites by fluorescence titration with thioflavin T

When thioflavin T binds to the AChE P-site its fluorescence is enhanced nearly 1000-fold, and the enhanced fluorescence is partially quenched when a second ligand binds to the A-site in a ternary complex (7). In experiments with thioflavin T and AChE alone, the fluorescence (F) was recorded over 3 – 4 min intervals in the Hi-Tech SFA 20 stopped flow apparatus described above for improved F stability. Average F values were corrected for inner filter effects (18) as described previously (12). Data were consistent with a single thioflavin T binding site on AChE and analyzed with eq. 2, a slight extension of a previous equation (7).

$$F=F_B+0.5(f_{EL} - f_Q) \cdot \left[D - \sqrt{D^2 - 4[E]_{tot}[L]_{tot}} \right]$$

(eq. 2)

In eq. 2, $D = [E]_{tot} + [L]_{tot} + K_L$, where $[E]_{tot}$ and $[L]_{tot}$ are the total enzyme and thioflavin T concentrations, respectively, and K_L is the equilibrium dissociation constant; $F_B = B + f_Q[L]_{tot} + f_E[E]_{tot}$, where B is the blank fluorescence without E or L and $f_Q = f_L/(1 + ([L]_{tot}/K_Q))$; and f_L, f_{EL} and f_E are the fluorescence intensity coefficients for free thioflavin T, bound thioflavin T, and free enzyme, respectively. Values of f_L, f_E, B and K_Q were determined from measurements with thioflavin T or enzyme alone. The parameter K_Q was introduced here to account for slight self-quenching at high concentrations of thioflavin T. Data were fitted to eq. 2 by unweighted nonlinear regression analysis (Fig.P version 6.0c), with $[L]_{tot}$ as the independent variable and K_L and f_{EL} as the fitted parameters.

Thioflavin T fluorescence was also employed to evaluate the interactions of carbachol (S) at the A- and P-sites. In the context of Scheme 2, the expression for the time dependence of F is given by eq. 3 (where $[EC] = 0$ at time $t = 0$). In eq. 3, F_0 is the fluorescence at time = 0 and F_F is the fluorescence when carbamoylation has reached a final steady state.

$$F=F_0+(F_F - F_0)\left(1 - e^{-[(k_{12}+k_{21})t]}\right)$$

(eq. 3)

Examination of k_{12} and k_{21} again will largely be deferred here in order to focus on the useful thermodynamic information obtained by measuring F_0 over a range of ligand concentrations. Since analysis of F_0 assumed no carbamoylated enzyme EC at time $t = 0$, the relevant species from Scheme 2 and the new species with thioflavin T bound to the P-site are given in Scheme 3.

In Scheme 3 the affinity of thioflavin T (L) at the P-site (denoted by subscript P) of AChE is characterized by the dissociation constant K_L in the absence of carbachol (S) and by $i_2 K_L$ when S occupies the A-site. All reactions were assumed to reach equilibrium, and analysis of the F_0 data was based on eq. 4, a slightly rewritten form of a previous equation (12).

$$F_0 = F_B + \frac{[E]_{tot} \quad f_{EL} \cdot \frac{[L]}{K_L} \cdot \left[1 + \left(\frac{f_{ELS}}{f_{EL}} \right) \left(\frac{[S]}{i_2 K_M} \right) \right]}{1 + \frac{[S]}{K_{M+S}} + \frac{[L]}{K_L} + \frac{[S]}{K_M} \cdot \left[\frac{[S]}{iK_S} + \frac{[L]}{i_2 K_L} \right]}$$

(eq. 4)

In eq. 4, $F_B = B + f_L[L] + f_S[S]$, where B is the blank fluorescence with E in the absence of L or S, and it is assumed that $[L] \cong [L]_{tot}$ and $[S] \cong [S]_{tot}$. Values of f_L and f_S were determined from measurements with thioflavin T or carbachol alone and K_L was obtained with eq. 2. The coefficients f_{EL} and f_{ELS} denote the fluorescence of thioflavin T in the binary complex E_L and the ternary complex ELS, respectively. K_M is equal to $K_S K_1$ and K_{M+S} is given in eq. 5.

$$\frac{[S]}{K_{M+S}} = \frac{i[S]}{iK_S} + \frac{[S]}{K_M}$$

(eq. 5)

F_0 data were initially fitted to eq. 4 by nonlinear regression analysis (SigmaPlot version 10) with [S] as the independent variable, [L], f_L, K_L, i and i_2 as fixed parameters, and K_M, iK_S, f_{EL} and f_{EL}/f_{ELS} as the fitted parameters. Control reactions with AChE and thioflavin T alone were interspersed with runs that included carbachol to confirm the stability of f_{EL}. A second cycle of data fitting was then conducted in which multiple data sets, each at different fixed $[L]_{tot}$, were analyzed simultaneously in the SCoP program as described previously (7). In these simultaneous fits f_{EL} was added to the previously fixed parameters and either i or i_2 became one of the four fitted parameters. Replacement of K_M with K_{M+S} as one of the fitted parameters involved eliminating K_M with the substitution $K_M = K_{M+S}iK_S/(iK_S - (i)(K_{M+S}))$ (from eq. 5).

Results and Discussion

The fluorescence of thioflavin T was enhanced by a factor of more than 800 when it bound to AChE (Figure 2). The fluorescence increase was consistent with thioflavin T interaction at a single site in human AChE with an equilibrium dissociation constant of 1.9 µM, in good agreement with a previous determination of 0.9 µM obtained at a somewhat lower ionic strength (7). The structure of the thioflavin T complex with TcAChE obtained by X-ray crystallography indicates that the ligand binds to the AChE P-site, with the benzothiazole ring of thioflavin T stacked against Trp279 and its dimethylaminophenyl moiety 3.5Å distant from and nearly coplanar with the phenyl group of Phe330 (19). The two rings of thioflavin T are planar, and this loss of rotational mobility is thought to provide the fluorescence enhancement in thioflavin T-AChE complexes (20). The partial quenching of this fluorescence when an A-site ligand binds to form a ternary complex can also be explained by three-dimensional structures. In crystal structures of TcAChE with two ligands specific for the A-site, edrophonium (21) and TMTFA (9), the phenyl ring of Phe330 is rotated ~115° relative to its position in the thioflavin T-TcAChE complex. In this orientation, the phenyl ring would partially overlap with the crystal structure location of thioflavin T. Therefore, the proximity of the phenyl ring is likely to slightly distort the planarity of thioflavin T and decrease the fluorescence in the ternary complex.

The difference in thioflavin T fluorescence intensity between these binary and ternary complexes allows the binding of both A and P-site ligands to be quantified (7,12). To apply this approach to the reaction of carbachol with recombinant human AChE, we first compared recordings obtained with acetylthiocholine or thioflavin T. Because carbamates are poor substrates that form a slowly hydrolyzed EC intermediate (Scheme 1–Scheme 3), their reaction progress is usually monitored by changes in AChE activity with a reporter substrate like acetylthiocholine at discrete time points. Only a few studies have attempted to continuously

follow the reaction in the presence of both carbamate and reporter substrate. Examples of absorbance traces produced when carbachol (S_1) and acetylthiocholine (S_2) were rapidly mixed with AChE in a stopped flow apparatus are shown in Figure 3. Initial acetylthiocholine hydrolysis rates progressively decreased as AChE was carbamoylated until a final, relatively slow steady-state hydrolysis rate was attained. This approach has the advantage that both the carbamoylation and decarbamoylation rate constants (k_{12} and k_{21}, respectively) can be obtained together as described under eq. 1. Preliminary analyses of these rate constants has been reported (14), and more refined analyses are in progress (T. L. Rosenberry, manuscript in preparation).

Fluorescence changes when carbachol was rapidly mixed with the binary complex of thioflavin T and AChE depended on the carbachol concentration (Figure 4). With 0.5 mM carbachol, the fluorescence decreased about 30% over a time course comparable to that observed for the initial decrease in acetylthiocholine hydrolysis rates with 0.6 mM carbachol in Figure 3. At a higher 10 mM concentration of carbachol, almost no fluorescence change was observed during the reaction, and at 60 mM carbachol a rapid slight increase in fluorescence was observed (Figure 4). Thioflavin T can bind to both E and EC, and the direction of the fluorescence change depended on the relative quenching of complexes formed by E and EC. Estimates of k_{12} became imprecise when there was little change in fluorescence during the reaction, compounding the fact that the signal-to-noise ratio was somewhat higher for reactions monitored with acetylthiocholine than with thioflavin T at all carbachol concentrations. However, the fluorescence measurements have one significant advantage, namely that the initial fluorescence F_0 and the final fluorescence F_F can be analyzed as in Scheme 3 and eq. 4 to obtain carbachol equilibrium binding constants.

Values of F_0 in Figure 4 decreased progressively with increasing carbachol concentration, consistent with the expected partial quenching of thioflavin T fluorescence in the reversible ternary complex formed when carbachol binds to the A-site in the ternary complex involving E. However, analysis of the F_0 data is challenging. Scheme 3 includes four independent equilibrium constants for carbachol binding (K_M, iK_S, i and i_2), and it is difficult for an F_0 analysis to uniquely assign all four. F_0 was obtained as a function of the carbachol concentration from traces like those in Figure 4 in three experiments, each at a different fixed concentration of thioflavin T, and these data sets were fitted to eq. 4 as outlined in the Experimental Methods (Figure 5). Analyses of the individual data sets indicated that f_{EL} was invariant but that the other fitted values depended on the values assigned to i and i_2 (as found previously with thioflavin T and the substrate ATMA, 12). The dependence on i and i_2 was reduced when the multiple data sets were analyzed simultaneously in the SCoP program. We previously showed that the equilibrium constants corresponding to K_M and i_2 for the binding of the specific A-site ligand edrophonium in its binary complex with E and its ternary complex with E and thioflavin T could be assigned unambiguously from a similar combination of fluorescence data sets (7). However, edrophonium does not show significant binding to the P-site (equivalent to eliminating ESS$_P$ in Scheme 3 and to setting $iK_S{}^{-1} = 0$ and eliminating i as a variable in eq. 4). Results from the simultaneous fitting in Figure 5 are shown in Table 1, and they indicate that some but not all of the fitted parameters for carbachol binding became invariant. The two invariant parameters are f_{EL}/f_{ELS} and K_{M+S}, a measure of the overall binding of carbachol to the A- and P-sites (see eq. 5). Ranges for the other fitted parameters are shown in the last two rows of Table 1. These ranges are dictated by the requirements that i be positive (fixing i_2 at a maximum of 1.12) and that $iK_S > K_M$ (fixing i_2 at a minimum of 0.40). These are very conservative requirements. Based on previous estimates of i_2 with edrophonium (1.12, 7) and ATMA (3.1, 12), it is unlikely that either i or i_2 with carbachol is much less than 1.0. A reasonable best estimate is to fix i_2 at 0.90, which leads to the fitted parameters in the top row of Table 1 and suggests that the probable range of K_M, iK_S and i_2 is within 20% of their values in this row. Slightly more uncertainty surrounds i, as its value is determined by the level of ES$_P$, a very minor component in these titrations. However, it is likely to lie between 1 and a

maximal value of 1.96, obtained when i_2 was fixed at 0.56. Additional studies are required to determine whether even less ambiguity in these values can be achieved with simultaneous fitting of a greater number of data sets at different fixed concentrations of thioflavin T.

The parameter f_{EL}/f_{ELS} is a measure of the relative quenching of thioflavin T fluorescence in the ternary complex. Its value of 1.54 was invariant in Table 1 and was significantly smaller than f_{EL}/f_{ELS} with edrophonium (2.76 ± 0.02, 7) or ATMA (3.0 ± 0.2, 12). We contend above that this relative quenching arises from rotation of the phenyl ring of Phe330 in the ternary complex. The lower value of f_{EL}/f_{ELS} for carbachol therefore implies that carbachol binding to the A-site induces a smaller rotation of the phenyl ring of Phe330 and less distortion of the planarity of thioflavin T in the ternary complex.

Acknowledgements

References

1. Rosenberry, TL. Acetylcholinesterase. In: Meister, A., editor. Advances in Enzymology. New York: John Wiley & Sons; 1975. p. 103-218.

2. Giacobini, E. Cholinesterase inhibitors: from the Calabar bean to Alzheimer therapy. In: Giacobini, E., editor. Cholinesterases and Cholinesterase Inhibitors. London: Martin Dunitz; 2000. p. 181-226.

3. Millard CB, Broomfield CA. Anticholinesterases: medical applications of neurochemical principles. J. Neurochem 1995;64:1909–1918. [PubMed: 7722478]

4. Rosenberry TL. Quantitative simulation of endplate currents at neuromuscular junctions based on the reactions of acetylcholine with acetylcholine receptor and acetylcholinesterase. Biophys. J 1979;26:263–290. [PubMed: 262418]

5. Changeux J-P. Responses of acetylcholinesterase from *Torpedo marmorata* to salts and curarizing drugs. Mol. Pharmacol 1966;2:369–392. [PubMed: 5970686]

6. Taylor P, Lappi S. Interaction of fluorescence probes with acetylcholinesterase. The site and specificity of propidium binding. Biochemistry 1975:1989–1997. [PubMed: 1125207]

7. De Ferrari GV, Mallender WD, Inestrosa NC, Rosenberry TL. Thioflavin T is a fluorescent probe of the acetylcholinesterase peripheral site that reveals conformational interactions between the peripheral and acylation sites. J. Biol. Chem 2001;276:23282–23287. [PubMed: 11313335]

8. Sussman JL, Harel M, Frolow F, Oefner C, Goldman A, Toker L, Silman I. Atomic structure of acetylcholinesterase from *Torpedo californica*: A prototypic acetylcholine-binding protein. Science 1991;253:872–879. [PubMed: 1678899]

9. Harel M, Quinn DM, Nair HK, Silman I, Sussman JL. The X-ray structure of a transition state analog complex reveals the molecular origins of the catalytic power and substrate specificity of acetylcholinesterase. J. Am. Chem. Soc 1996;118:2340–2346.

10. Bourne Y, Taylor P, Marchot P. Acetylcholinesterase inhibition by fasciculin: Crystal structure of the complex. Cell 1995;83:503–512. [PubMed: 8521480]

11. Mallender WD, Szegletes T, Rosenberry TL. Organophosphorylation of acetylcholinesterase in the presence of peripheral site ligands: Distinct effects of propidium and fasciculin. J. Biol. Chem 1999;274:8491–8499. [PubMed: 10085081]

12. Johnson JL, Cusack B, Davies MP, Fauq A, Rosenberry TL. Unmasking tandem site interaction in human acetylcholinesterase. Substrate activation with a cationic acetanilide substrate. Biochemistry 2003;42:5438–5452. [PubMed: 12731886]

13. Rosenberry TL, Bernhard SA. Studies of catalysis by acetylcholinesterase: Fluorescent titration with a carbamoylating agent. Biochemistry 1971;10:4114–4120. [PubMed: 5168614]

14. Rosenberry TL, Johnson JL, Cusack B, Thomas J, Emani S, Venkatasubban KS. Interactions between the peripheral site and the acylation site in acetylcholinesterase. Chem. Biol. Interact 2005:157–158. 181–189.

15. Rosenberry TL, Bernhard SA. Studies on catalysis by acetylcholinesterase: Synergistic effects of inhibitors during hydrolysis of acetic acid esters. Biochemistry 1972;11:4308–4321. [PubMed: 5079901]

16. Brufani M, Lippa S, Marta M, Oradei A, Pomponi M. Acetylcholinesterase inhibition by eserine: rate constants of reaction. Part II. Ital. J. Biochem 1985;34:328–340. [PubMed: 4077467]

17. Szegletes T, Mallender WD, Rosenberry TL. Nonequilibrium analysis alters the mechanistic interpretation of inhibition of acetylcholinesterase by peripheral site ligands. Biochemistry 1998;37:4206–4216. [PubMed: 9521743]

18. Lakowicz, JR. Principles of Fluorescence Spectroscopy. 2nd ed. New York: Kluwer Academic/ Plenum; 1999. ed.

19. Harel, M.; Sonoda, LK.; Silman, I.; Sussman, JL.; Rosenberry, TL. J. Am. Chem. Soc. 2008. The crystal structure of thioflavin T bound to the peripheral site of *Torpedo californica* acetylcholinesterase reveals how thioflavin T acts as a sensitive fluorescent reporter of ligand binding to the acylation site. in press

20. Friedhoff P, Schneider A, Mandelkow EM, Mandelkow E. Rapid assembly of Alzheimer-like paired helical filaments from microtubule-associated protein tau monitored by fluorescence in solution. Biochemistry 1998;37:10223–10230. [PubMed: 9665729]

21. Harel M, Schalk I, Ehret-Sabatier L, Bouet F, Goeldner M, Hirth C, Axelsen PH, Silman I, Sussman JL. Quaternary ligand binding to aromatic residues in the active-site gorge of acetylcholinesterase. Proc. Natl. Acad. Sci. USA 1993;90:9031–9035. [PubMed: 8415649]
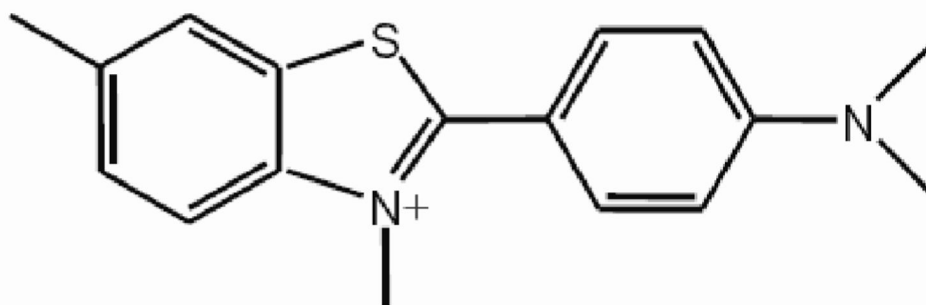
Figure 1.
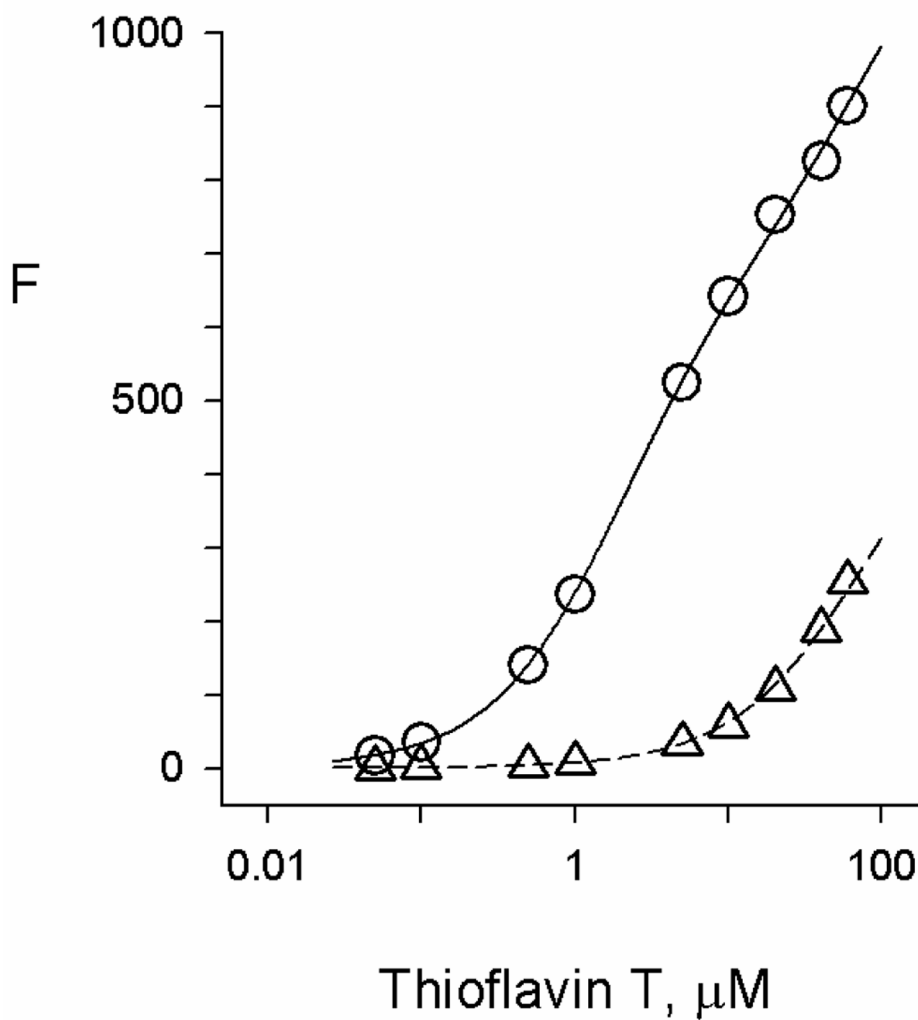Structure of thioflavin T.

Figure 2.
Fluorescence titration of AChE with thioflavin T. Fluorescence values (F) were measured as outlined in the Experimental Methods at the indicated total concentrations of thioflavin T. The fluorescence intensity coefficient for the free ligand (f_L) was obtained from the plot in the absence of AChE (Δ). The fluorescence F in the presence of a fixed concentration of AChE (110 nM) (O) was then analyzed as outlined in the Experimental Methods. Average values from four experiments were $K_L = 1.91 \pm 0.18$ μM and $f_{EL}/f_L = 846 \pm 27$.
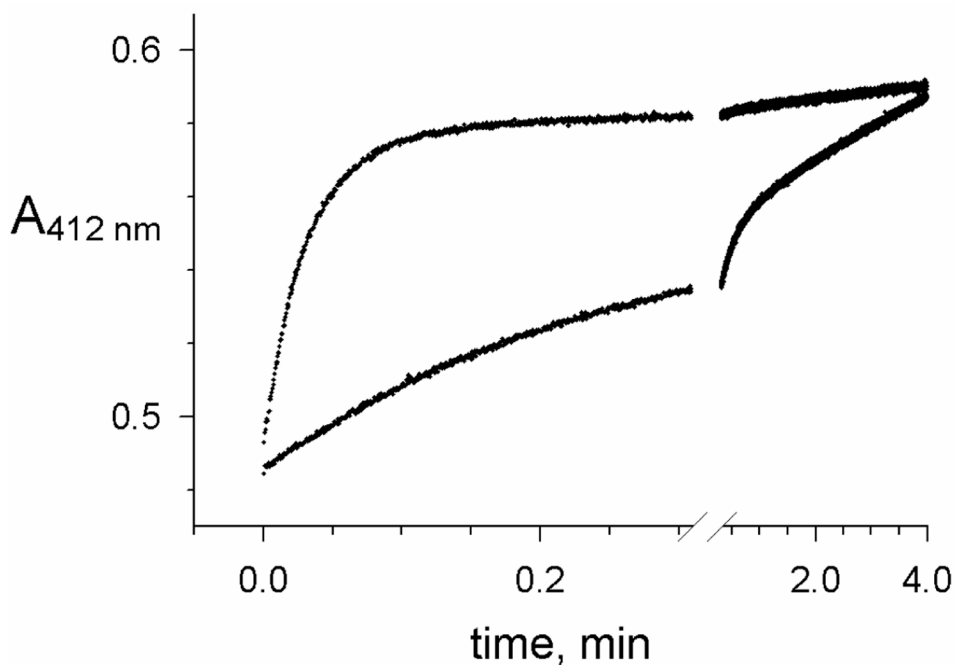
Figure 3.
Reactions of carbachol with AChE monitored by simultaneous hydrolysis of acetylthiocholine. Reactions were initiated by stopped-flow mixing of AChE with carbachol, acetylthiocholine, and DTNB as outlined in the Experimental Procedures. Initial concentrations of acetylthiocholine (58 µM) and DTNB (10 mM) were the same in each reaction, while the respective concentrations of carbachol and AChE were 0.6 mM and 0.57 nM (lower trace), and 60 mM and 120 nM (upper trace). Each trace was fitted to Scheme 1 by numerical integration to obtain values of k_{12}, k_{21} and v_0 as outlined in the Experimental Procedures. For the lower trace, $k_{12} = 3.7$ min^{-1} and $k_{21} = 0.16$ min^{-1}, while for the lower trace $k_{12} = 30$ min^{-1} and $k_{21} = 0.026$ min^{-1}, values consistent with a preliminary report (14). Total hydrolysis of 58 µM acetylthiocholine in the absence of carbachol gave an increase in A$_{412\,nm}$ of 0.25.
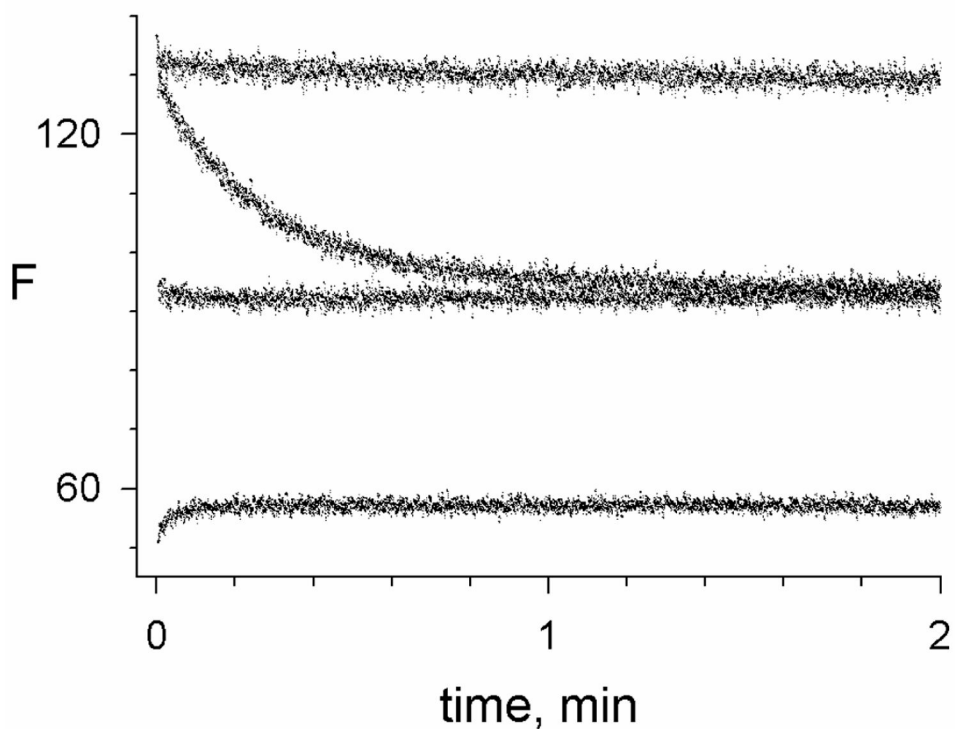
Figure 4.
Reactions of carbachol with AChE monitored by thioflavin T fluorescence. Reactions were
initiated by stopped-flow mixing of AChE with carbachol and thioflavin T as outlined in the
Experimental Procedures. Initial concentrations of thioflavin T (1.0 µM) and AChE (76 nM)
were the same in each reaction, while the respective concentrations of carbachol were 0, 0.5,
10 and 60 mM (from the upper to the lower trace). Each trace was fitted to eq. 3 by numerical
integration to obtain values of F_0, F_F, and $k_{12} + k_{21}$ as outlined in the Experimental Procedures.
For 0.5 and 60 mM carbachol, $k_{12} + k_{21} = 3.9$ and ~35 min^{-1}, respectively.
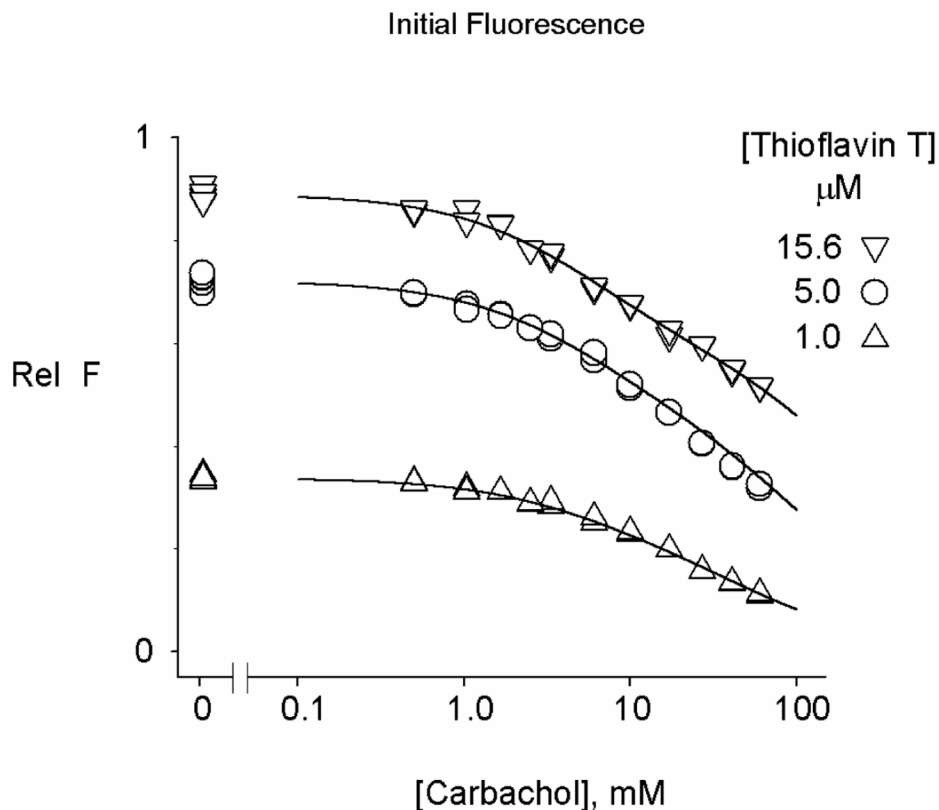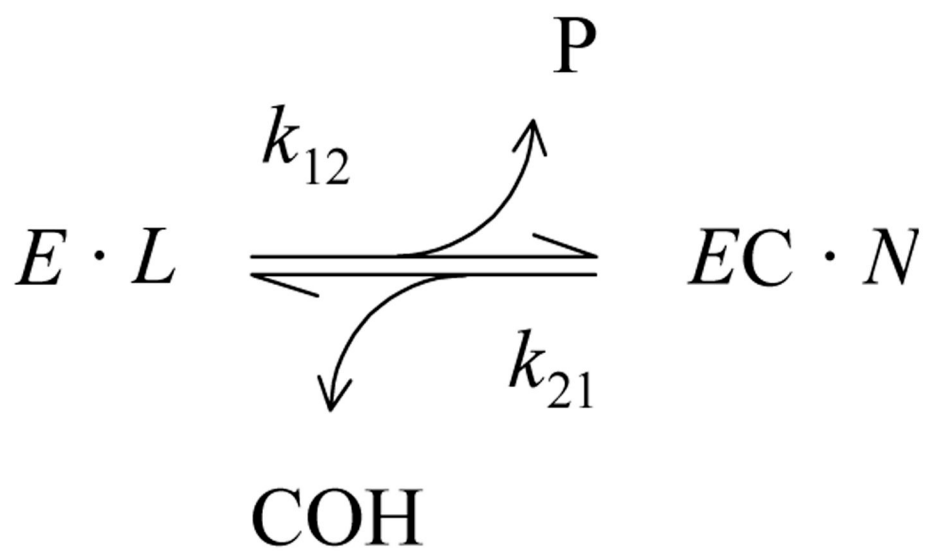
Figure 5.
Initial carbachol binding decreases the fluorescence of AChE-bound thioflavin T. The F_0 values of mixtures of AChE (70 – 155 nM), thioflavin T (1.0 – 15.6 µM, as noted), and the indicated concentration of carbachol were determined from stopped-flow traces like those in Figure 4. All the F_0 data were fitted simultaneously to Scheme 3 and eq. 4 as described in the Experimental Methods. The fluorescence blank F_B without AChE was determined in parallel measurements. Data are shown as normalized values (Rel F) corresponding to $(F_0 - F_B)/((f_{EL})(E_{tot}))$. Parameters obtained from the data fitting are shown in Table 1.

$$P$$

$$k_{12}$$

$$E \cdot L \; \rightleftharpoons \; EC \cdot N$$

$$k_{21}$$

$$COH$$

Scheme 1.

$$E + S \underset{}{\overset{K_S}{\rightleftharpoons}} ES_P \underset{}{\overset{K_1}{\rightleftharpoons}} ES \overset{k_2}{\rightarrow} EC + P \overset{k_3}{\rightarrow} E + COH$$

$$+ \qquad\qquad +$$

$$S \qquad\qquad S$$

$$iK_S \Updownarrow \qquad K_S \Updownarrow$$

$$ESS_P \overset{ak_2}{\rightarrow} ECS_P + P \overset{bk_3}{\rightarrow} ES_P + COH$$

Scheme 2.

$$
\begin{array}{ccc}
E\mathrm{L_P} & & E\mathrm{SL_P} \\
+ & & + \\
\mathrm{L} & & \mathrm{L} \\
K_\mathrm{L} \Updownarrow & & i_2 K_\mathrm{L} \Updownarrow \\
\end{array}
$$

$$
E + \mathrm{S} \overset{K_\mathrm{S}}{\rightleftharpoons} E\mathrm{S_P} \overset{K_1}{\rightleftharpoons} E\mathrm{S} + \mathrm{S} \overset{iK_\mathrm{S}}{\rightleftharpoons} E\mathrm{SS_P}
$$
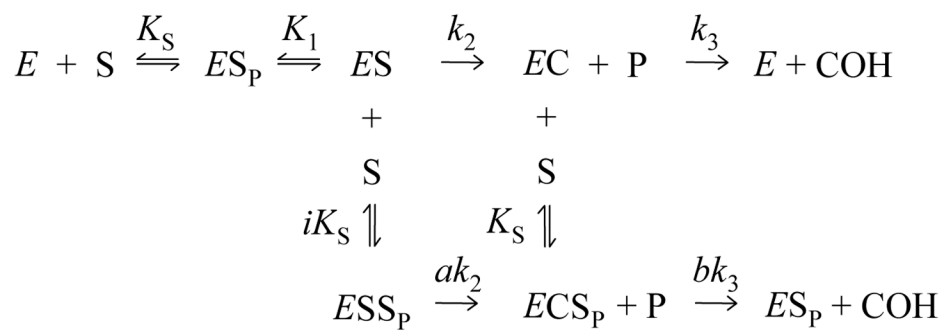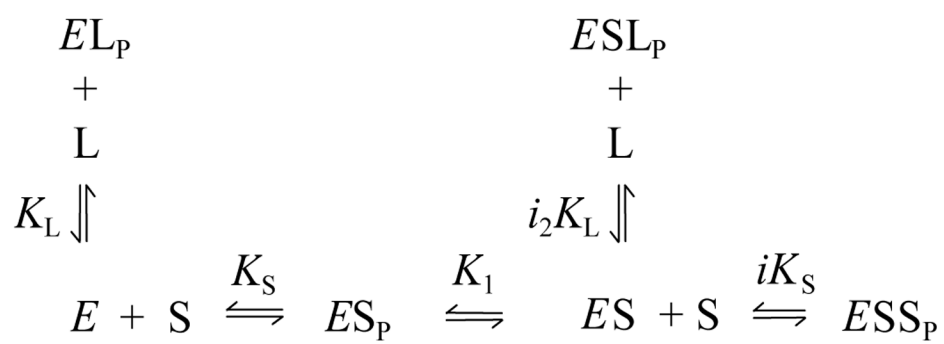
Scheme 3.

Table 1

Determination of carbachol binding to AChE from the thioflavin T fluorescence F_0.

	i_2	i	K_{M+S} mM	K_M mM	iK_s mM	f_{EL}/f_{ELS}
a	0.90 fixed	1.24	5.2 ± 0.3	6.5 ± 0.5	33 ± 4	1.54 ± 0.03
b	1.12	1e-6 fixed	5.24	5.24	41	1.54
b	0.40 fixed	1.80	5.24	15	15	1.54

K_L was fixed at 1.91 µM in all analyses. K_M was calculated from eq. 7.

[a] Simultaneous fit of the three data sets in Figure 5. Errors (SEM) were obtained by reanalyzing each data set individually with i fixed at 1.24, i_2 fixed at 0.90, and K_{M+S}, iK_S, f_{EL} and f_{EL}/f_{ELS} as the fitted parameters. Fitted parameter values from the three individual sets were then averaged and SEM was determined.

[b] Simultaneous fits of the three data sets in Figure 5 with fixed values selected to show maximum parameter range (see text).